Supplementary Information

Protein Interactions in the Murine Cytomegalovirus Capsid Revealed by CryoEM

Wong H. Hui[1,2], Qiyi Tang[3], Hongrong Liu[1,2,6], Ivo Atanasov[1,2], Fenyong Liu[4], Hua Zhu[5], Z. Hong Zhou[1,2,*]

[1]The California NanoSystems Institute (CNSI), University of California, Los Angeles (UCLA), Los Angeles, CA 90095-1594, USA

[2]Department of Microbiology, Immunology & Molecular Genetics, UCLA, Los Angeles, CA 90095-736422, USA

[3]Department of Microbiology/AIDS program, Ponce School of Medicine
395 Zona Industrial Reparadara-2, Ponce, PR 00716-2348, Puerto Rico

[4] School of Public Health, University of California at Berkeley, Berkeley, CA 94720, USA

[5]Department of Microbiology and Molecular Genetics, International Center for Public Health (or ICPH), Room E350D, 225 Warren Street, UMDNJ-New Jersey Medical School, Newark, NJ 07103-3506, USA

[6]Current address: College of Physics and Information Science, Hunan Normal University, 36 Lushan Road, Changsha, Hunan 410081, China

Running title: Murine cytomegalovirus capsid structure

Key words: cytomegalovirus; herpes simplex virus type 1; cryo electron microscopy; three-dimensional; major capsid protein.

[*]To whom correspondence should be addressed.

E-mail: Hong.Zhou@ucla.edu.

Tel: 310-983-1033

Legends of Supplemental Figures:

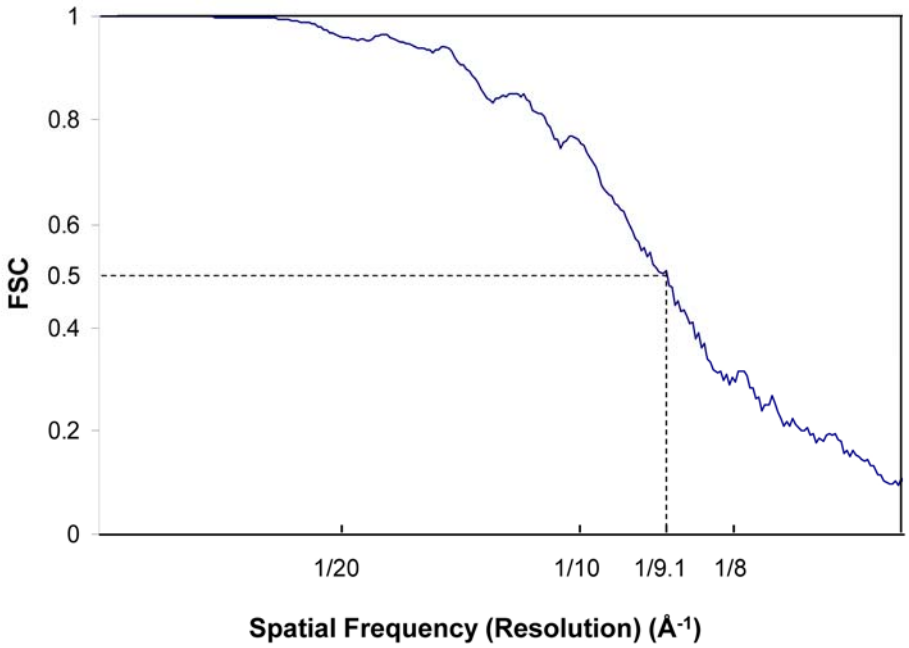

Fig. S1

Figure S1. Fourier shell correlation (FSC) curve. The estimated resolution of the MCMV capsid is 9.1 Å at FSC = 0.5.

Fig. S2

Figure S2. Sequence Alignment of MCPud of HSV-1 and MCMV

Alignment of sequence between the MCP upper domain of MCMV with HSV-1, obtained from the Pfam Sequence Search server (Finn et al., 2010) (http://pfam.sanger.ac.uk/search). Only the results corresponding to residues of HSV-1 MCPud (aa 484 to 1045) are shown. The section which is discussed in Figure 2 is highlighted in red.

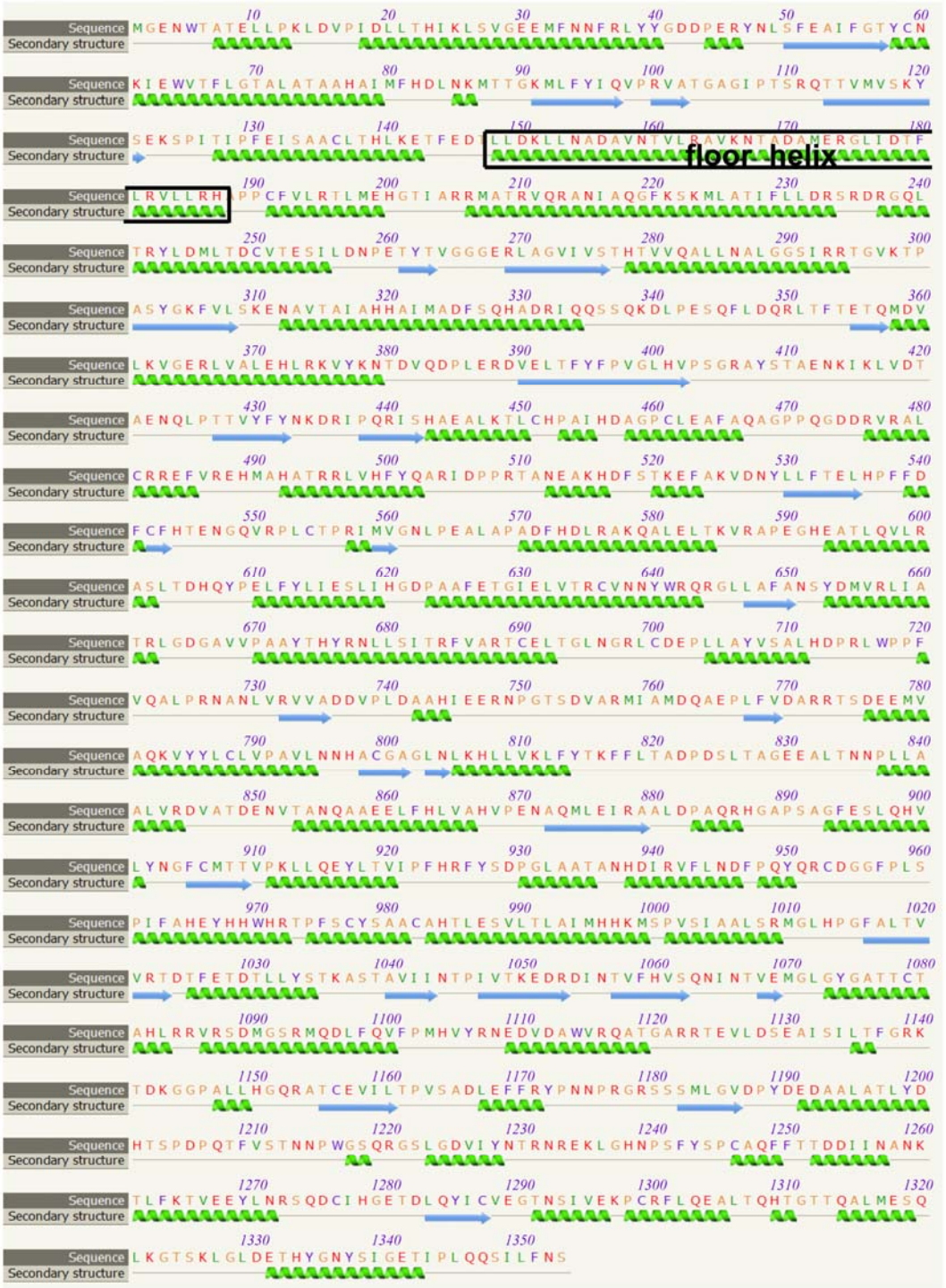

Fig. S3

Figure S3. Secondary structures of MCMV MCP. The prediction was carried out by three different prediction servers (Jpred Secondary Structure Prediction Server (Cole et al., 2008), PsiPred Protein Structure Prediction Server (Buchan et al., 2010) and Phyre^2 Protein Fold Recognition Server) and only the results from Phyre^2 Protein Fold Recognition Server (http://www.sbg.bio.ic.ac.uk/phyre2/html/page.cgi?id=index) are shown. Green helical ribbon: helix; blue arrow: β strand; grey line: loop.

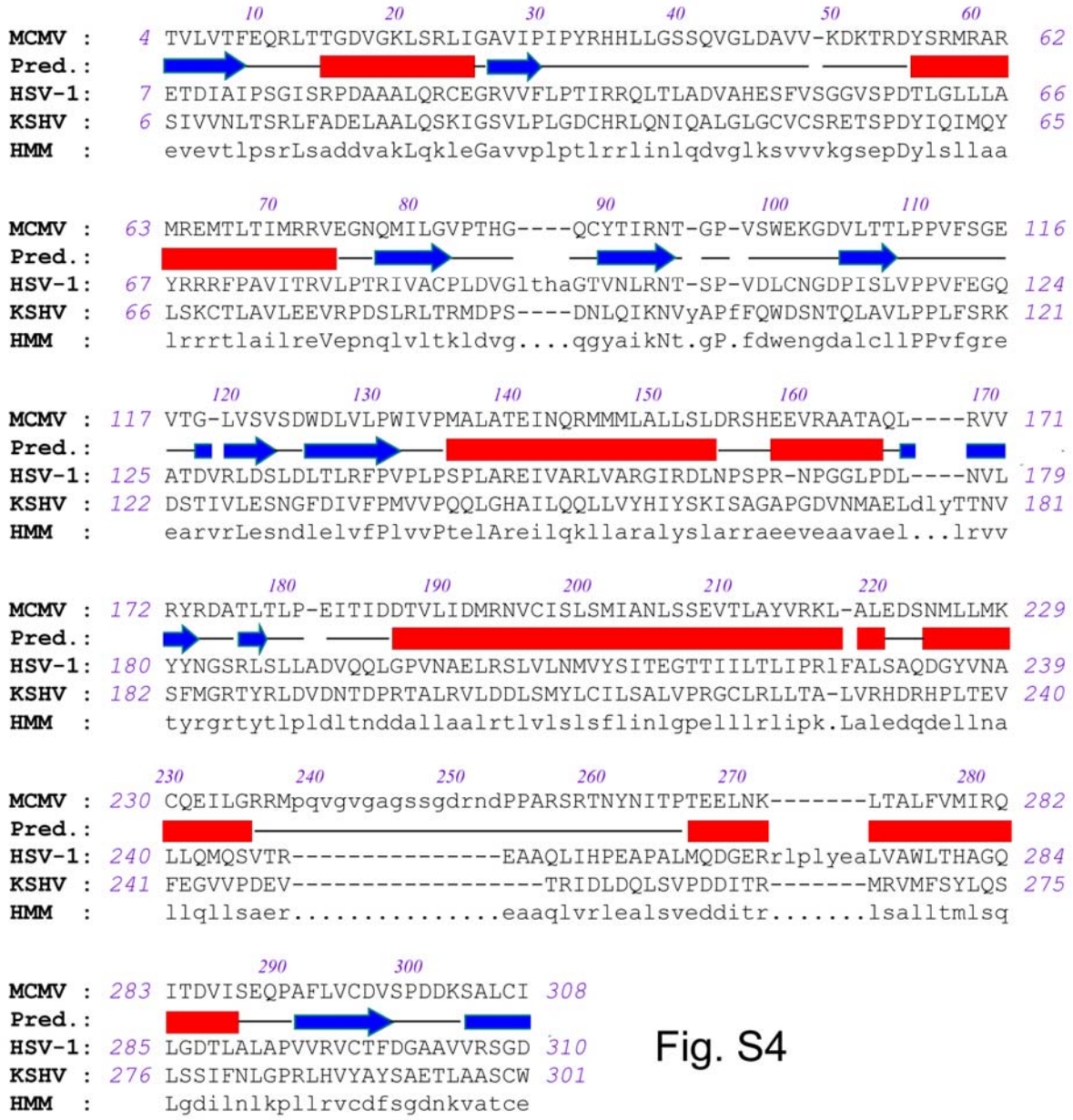

Fig. S4

Figure S4. Multi-sequence alignment of TRI-2 protein homologs across three herpesvirus subfamilies: MCMV M85, HSV-1 VP23, KSHV ORF26 and secondary structure prediction of MCMV TRI-2. Secondary structure prediction of MCMV TRI-2 by the PsiPred Protein Structure Prediction Server (Buchan et al., 2010) (http://bioinf.cs.ucl.ac.uk/psipred/) and are depicted in the second row. Red box: helix; blue arrow: β strand; black line: loop. The Hidden Markov Model (HMM) of the alignment generated by the Pfam server is shown in the last row. Numbers indicate amino-acid residual numbers in each sequence. Dashed lines in the sequences (dotted lines in the HMM model) represent deletions.

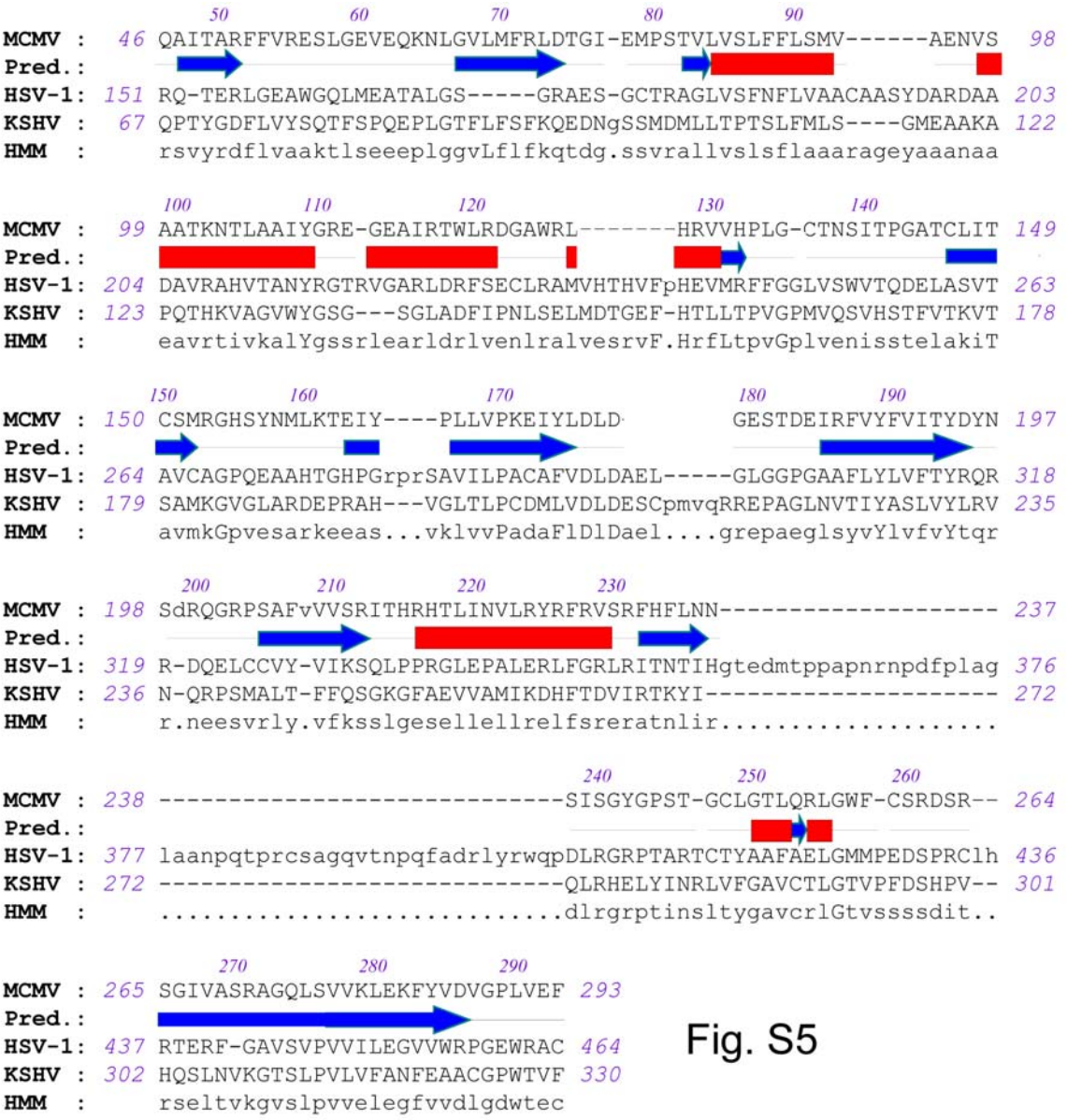

Fig. S5

Figure S5. Multi-sequence alignment of TRI-1 protein homologs in three herpesvirus subfamilies: MCMV M46, HSV-1 VP19c, KSHV ORF62 and secondary structure prediction of MCMV TRI-1. The secondary structures of MCMV TRI-1 was predicted by PsiPred server (Buchan et al., 2010) (http://bioinf.cs.ucl.ac.uk/psipred/) and are depicted in the second row. Red box: helix; blue arrow: β strand; black line: loop. The HMM of the alignment generated by the Pfam server (Finn et al., 2010) is shown in the last row. Numbers indicate the residual numbers in each protein. Dashed lines in the sequences (dotted lines in the HMM model) represent deletions.

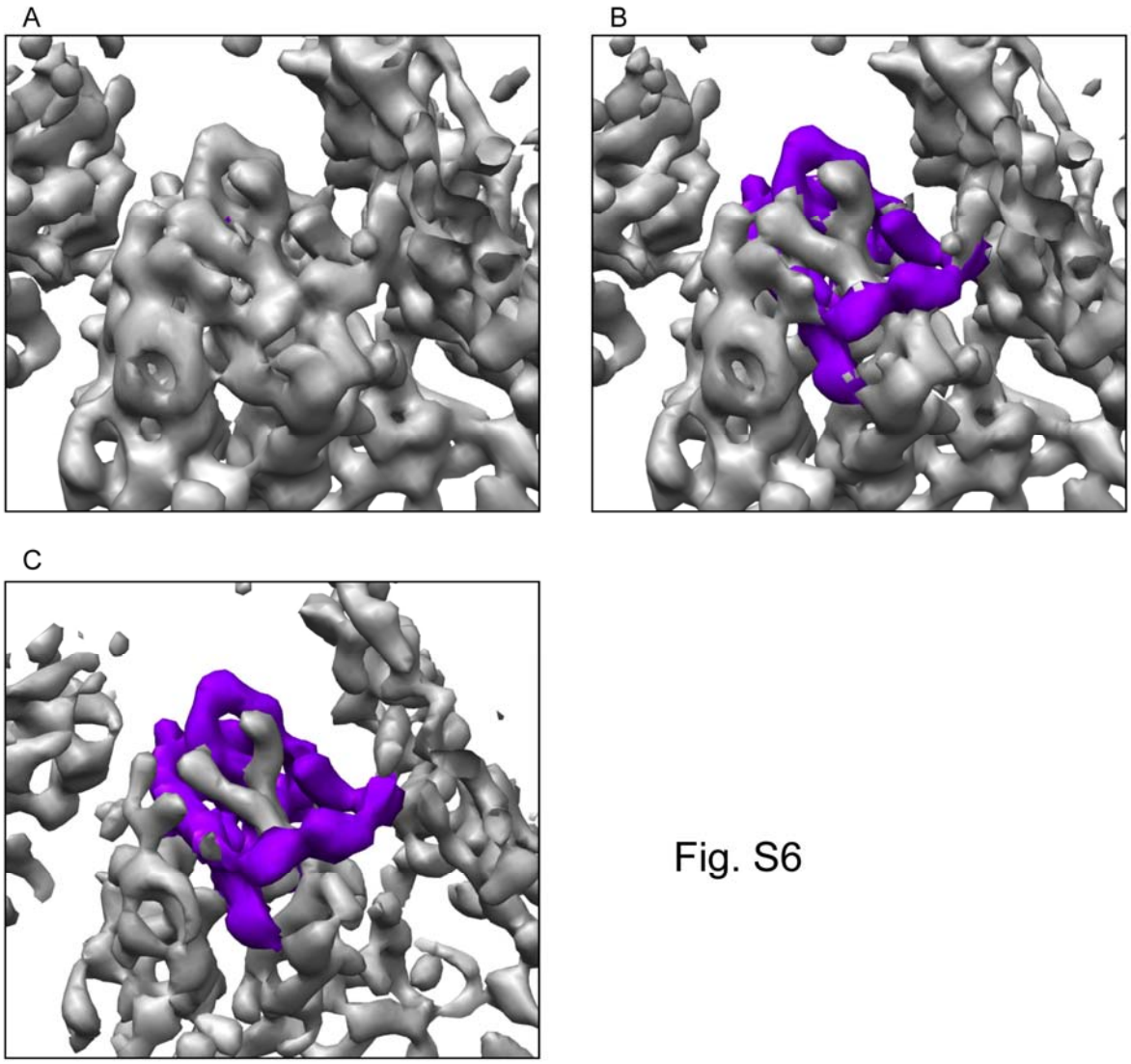

Figure S6. Estimation of molecular boundaries by varying density threshold for display. The averaged triplex density map was shown at three different density threshold values of 3.0 (A), 3.4 (B) and 4.5 (C). The densities corresponding to TRI-2a (purple) begin to be resolved from the rest of densities when the threshold density is above 3.4. This threshold-based estimation was used in conjunction with other available constraints to establish the final boundaries (see text).

Legends for Supplementary Movies:

Movie 1: MCMV Capsid Map from 3-fold View.

Radially color-shaded surface representation of the MCMV capsid reconstruction at ~9.1 Å resolution. One half of the full map is rotated, revealing hexons, pentons, triplexes arranged according to T=16 icosahedral symmetry on the capsid.

Movie 2: Fitting of cryoEM density of MCMV MCP with atomic models of HSV-1 MCPud and with the pseudo-atomic model of MCMV MCPud.

The cryoEM density map is shown in semitransparent gray, then the X-ray model of HSV-1 MCPud (ribbon with red helices) is superimposed, followed by the pseudo-atomic model of the MCMV MCPud (ribbon with purple helices).

Movie 3: Structure of triplex heterotrimer. Related to Fig. 4.

A triplex heterotrimer, is shown first, followed by separation of its three subunits, TRI-1 (magenta), TRI-2a (green), TRI-2b (yellow) individually, to reveal interactions among these subunits.

Movie 4: Interaction between triplex and its adjacent hexons. Related to Fig 5.

A triplex and its three associated hexons are shown together to reveal interactions between triplex heterotrimer and MCP.